AD-A169 796 COMPUTATION OF THE AMPLITUDE OF STRESS SINGULAR TERMS FOR CRACKS AND REEN..(U) WASHINGTON UNIV ST LOUIS MO CENTER FOR COMPUTATIONAL MECHANIC.. B A SZABO ET AL. 1/1

UNCLASSIFIED FEB 86 WU/CCM-86/1 N00014-85-K-0169 F/G 20/11 NL

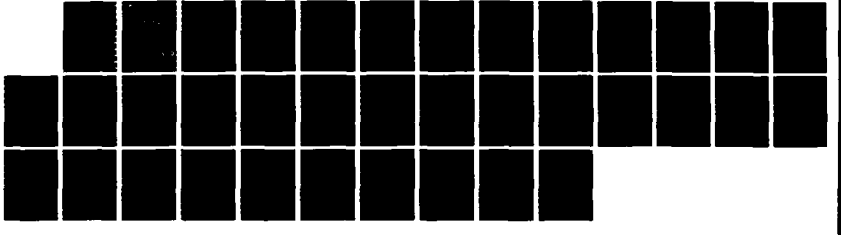

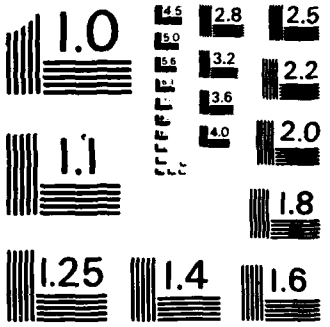

WASHINGTON UNIVERSITY IN ST. LOUIS

15

AD-A169 796

Report WU/CCM-86/1

COMPUTATION OF THE AMPLITUDE OF STRESS SINGULAR TERMS FOR CRACKS AND REENTRANT CORNERS

B. A. Szabo
Washington University

I. Babuska
University of Maryland

February 1986

CENTER FOR COMPUTATIONAL MECHANICS

WASHINGTON UNIVERSITY
CAMPUS BOX 1129
ST. LOUIS, MO 63130

3

REPORT DOCUMENTATION PAGE

READ INSTRUCTIONS BEFORE COMPLETING FORM

1. REPORT NUMBER: WU/CCM-86/1	2. GOVT ACCESSION NO.
3. RECIPIENT'S CATALOG NUMBER	
4. TITLE (and Subtitle): Computation of the Amplitude of Stress Singular Terms for Cracks and Re-entrant Corners	5. TYPE OF REPORT & PERIOD COVERED: Final life of contract
6. PERFORMING ORG. REPORT NUMBER	
7. AUTHOR(s): B. A. Szabo (Washington University); I. Babuska	8. CONTRACT OR GRANT NUMBER(s): AFOSR 82-0315; ONR N00014-85-K-0169
9. PERFORMING ORGANIZATION NAME AND ADDRESS: Center for Computational Mechanics, Washington University, Campus Box 1129, St. Louis, MO 63130	10. PROGRAM ELEMENT, PROJECT, TASK AREA & WORK UNIT NUMBERS
11. CONTROLLING OFFICE NAME AND ADDRESS: Department of Naval Research, Office of Naval Research, Arlington, VA 22217	12. REPORT DATE: February 1986
	13. NUMBER OF PAGES: 33
14. MONITORING AGENCY NAME & ADDRESS(if different from Controlling Office)	15. SECURITY CLASS. (of this report)
	15a. DECLASSIFICATION/DOWNGRADING SCHEDULE

16. DISTRIBUTION STATEMENT (of this Report)

Approved for public release: distribution unlimited

17. DISTRIBUTION STATEMENT (of the abstract entered in Block 20, if different from Report)

18. SUPPLEMENTARY NOTES

19. KEY WORDS (Continue on reverse side if necessary and identify by block number)

Finite element methods, p-extension, fracture mechanics, elasticity, stress intensity factors, mixed mode, extraction methods, convergence, error estimate.

20. ABSTRACT (Continue on reverse side if necessary and identify by block number)

The theoretical basis and performance characteristics of two new methods for the computation of the coefficients of the terms of asymptotic expansions at reentrant corners from finite element solutions are presented. The methods, called the countour integral method and the cutoff function method, are very efficient. Numerical examples are given.

Report No. WU/CCM-86/1

COMPUTATION OF THE AMPLITUDE OF STRESS SINGULAR TERMS FOR CRACKS AND REENTRANT CORNERS.

Barna A. Szabó

Albert P. and Blanche Y. Greensfelder Professor of Mechanics and Director, Center for Computational Mechanics
Washington University in St. Louis

Ivo Babuška

Research Professor, Institute for Physical Science and Technology
University of Maryland, College Park, Maryland

February, 1986.

Prepared for presentation at the
Nineteenth National Symposium on Fracture Mechanics
San Antonio, Texas
June 30-July 2, 1986

ABSTRACT

The theoretical basis and performance characteristics of two new methods for the computation of the coefficients of the terms of asymptotic expansions at reentrant corners from finite element solutions are presented. The methods, called the *contour integral method* and the *cutoff function method*, are very efficient: The coefficients converge to their true values as fast as the strain energy, or faster.

In order to make the presentation as simple as possible, we assume that the elastic body is homogeneous and isotropic, is loaded by boundary tractions only and, in the neighborhood of the reentrant corner, its boundaries are stress free. The methods described herein can be adapted to cases without such restrictions.

KEYWORDS

Finite element methods, p-extension, fracture mechanics, elasticity, stress intensity factors, mixed mode, extraction methods, convergence, error estimate.

TABLE OF CONTENTS.

1. INTRODUCTION.

Our understanding and ability to control the error of approximation in finite element computations has advanced very substantially in the last two years. Two developments are especially important: (1) Under assumptions which are generally satisfied in engineering computations, we are now able to realize *exponential* rates of convergence in any quantity of interest; and (2) using feedback information from finite element solutions we can ensure that the error in all quantities of interest is small. In this paper we describe two new methods for the computation of generalized stress intensity factors in two dimensional problems of linear elasticity and demonstrate their performance by examples.

We will restrict our attention to the displacement formulation. We denote the solution domain by Ω and the displacement vectors defined on Ω by $\vec{u}$ or (equivalently) $\{u\}$:

$$\vec{u} \equiv \{u\} \stackrel{\text{def}}{=} \{u_x(x,y)\ u_y(x,y)\}. \tag{1.1}$$

We denote the work done on the elastic body by the stresses corresponding to $\vec{u}$ when the elastic body is subjected to displacements $\vec{v}$ by $B(\vec{u},\vec{v})$; the strain energy by $U(\vec{u})$ and the potential energy by $\Pi(\vec{u})$. Note that $2U(\vec{u}) = B(\vec{u},\vec{u})$. We denote the set of all displacement vector functions defined on Ω for which $U(\vec{u}) < \infty$ by $E(\Omega)$ and associate the energy norm with this set:

$$\|\vec{u}\|_{E(\Omega)} \stackrel{\text{def}}{=} \sqrt{U(\vec{u})} \equiv \sqrt{\frac{1}{2} B(\vec{u},\vec{u})}. \tag{1.2}$$

We denote the set of all admissible displacement functions by $\tilde{E}(\Omega)$. By definition, a displacement function $\vec{u}$ is admissible if it has finite strain energy and on those boundary segments of Ω where one or both displacement components is prescribed the components of $\vec{u}$ equal the prescribed displacement components values. That is:

$$\tilde{E}(\Omega) \stackrel{\text{def}}{=} \left\{ \vec{u} \,|\, \vec{u} \in E(\Omega);\ u_x(P) = \tilde{u}_x(P),\ P \in \partial\Omega_x^{(D)};\ u_y(P) = \tilde{u}_y(P),\ P \in \partial\Omega_y^{(D)} \right\} \tag{1.3}$$

where $\tilde{u}_x$, $\tilde{u}_y$ are prescribed displacement components and $\partial\Omega_x^{(D)}$ (resp. $\partial\Omega_y^{(D)}$) represents those boundary segments where u_x (resp. u_y) is prescribed. The exact solution of the generalized formulation of a problem of plane elasticity $\vec{u}_{EX}$ satisfies:

$$\Pi(\vec{u}_{EX}) = \min_{\vec{u} \in \tilde{E}(\Omega)} \Pi(\vec{u}). \tag{1.4}$$

In finite element analysis we seek to approximate $\vec{u}_{EX}$. We do this by constructing a finite element mesh Δ on Ω. Each quadrilateral (resp. triangular) finite element is mapped onto a standard quadrilateral (resp. triangular) finite element by suitable mapping functions. We define sets of basis functions on the standard triangular and quadrilateral elements so that any polynomial of degree p or less defined as the standard element can be written as a linear combination of the basis function.

The polynomial basis functions defined on the standard element are mapped onto the elements of the mesh Δ and are joined to form a set of basis functions on Ω. These basis functions are continuous across interelement boundaries but no restrictions are imposed on their derivatives across interelement boundaries. Thus the basis functions are *exactly and minimally conforming*. The basis functions defined on Ω are characterized by the mesh Δ, the polynomial degree p and the mapping functions Q. The set of functions that can be expressed by linear combination of the basis function is denoted by $S^p(\Omega, \Delta, Q)$ and called: *finite element space*. Because the basis functions are continuous across interelement boundaries, $S^p(\Omega, \Delta, Q)$ is a subset of $E(\Omega)$. We denote the set of admissible functions in $S^p(\Omega, \Delta, Q)$ by $\tilde{S}^p(\Omega, \Delta, Q)$. The number of basis functions in $\tilde{S}^p(\Omega, \Delta, Q)$ is called the *number of degrees of freedom* and is denoted by N. The finite element solution $\vec{u}_{FE}$ satisfies:

$$\Pi(\vec{u}_{FE}) = \min_{\vec{u} \in \tilde{S}^p(\Omega, \Delta, Q)} \Pi(\vec{u}) \tag{1.5}$$

and has the following property:

$$\|\vec{u}_{EX} - \vec{u}_{FE}\|_{E(\Omega)} = \min_{\vec{u} \in \tilde{S}^p(\Omega, \Delta, Q)} \|\vec{u}_{EX} - \vec{u}\|_{E(\Omega)}. \tag{1.6}$$

The finite element method selects $\vec{u}_{FE}$ from $\tilde{S}^p(\Omega, \Delta, Q)$ on the basis of criterion (1.6). We can reduce the error of approximation by mesh refinement, increase of

the polynomial degree of elements, or a combination of both. These are called *extension processes.* If the polynomial degree of elements is fixed and the error of approximation is reduced by mesh refinement then the process is called *h-extension* (h refers to the size of the elements). If the mesh is fixed and the polynomial degree of elements (p) is increased then the process is called *p-extension.* We remark that neither the mesh refinement nor the distribution of polynomial degrees has to be uniform. There is a substantial improvement in performance* and no significant increase in computational overhead if properly designed meshes are used instead of uniform meshes. On the other hand there is no significant improvement in performance but there is a significant increase in computational overhead if graded p-distributions are used instead of uniform p-distributions. For this reason we will use uniform p-distributions, characterized by a single number, p. When the error of approximation is reduced so that mesh refinement is combined with increasing p then the extension process is called *h-p extension.*

In the case of h- and p-extensions the rate of convergence is *algebraic.* That is:

$$\| \vec{u}_{EX} - \vec{u}_{FE} \|_{E(\Omega)} \leq \frac{k}{N^{\beta}} \tag{1.7a}$$

where N is the number of degrees of freedom; k and β are positive constants, independent of N but dependent on $\vec{u}_{EX}$ and the finite element meshes. In the case of h-p extensions, when proper mesh refinement is used in conjunction with p-extension, the rate of convergence is *exponential:*

$$\| \vec{u}_{EX} - \vec{u}_{FE} \|_{E(\Omega)} \leq \frac{k}{\exp(\gamma N^{\theta})} \tag{1.7b}$$

where k, γ and θ are positive constants. Under certain assumptions which are generally satisfied in engineering applications $\theta \geq 1/3$.

Although it is difficult to write computer programs that automatically design meshes and assign polynomial degrees so that the rate of convergence (1.7b) is realized for all N, very similar performance can be achieved when properly graded,

* *In this context "performance" means: rate of change of error in energy norm with respect to the number of degrees of freedom.*

fixed meshes are used in conjunction with p-extension. In this case nearly exponential convergence rate is achieved for low N but convergence slows to an algebraic rate for high N. Clearly, the mesh should be designed so that the desired level of precision is achieved *before* the rate of convergence slows. Properly designed meshes are such that the sizes of elements decrease in geometric progression with a common factor of about 0.15 toward points of stress singularity. Selection of the mesh and the polynomial degree of elements depends on the accuracy one wishes to achieve. For details and examples see [1-8].

We are now in position to outline the central point of this paper: In [9] a new approach for the computation of functionals from finite element solutions was presented. In this approach a desired functional value $\Phi(\vec{u}_{FE})$ (e.g. a stress component at a point; stress intensity factor, etc.) is computed from an expression which is of the form:

$$\Phi(\vec{u}_{FE}) = B(\vec{u}_{FE}, \vec{v}) \tag{1.8}$$

where $\vec{v}$ is a suitably chosen function, called *extraction function*. Methods of this type are called *extraction methods*. In [10] it was shown that the error in the functional value computed by extraction methods can be written as:

$$|\Phi(\vec{u}_{EX}) - \Phi(\vec{u}_{FE})| \leq \|\vec{u}_{EX} - \vec{u}_{FE}\|_{E(\Omega)} \|\vec{\omega}_{EX} - \vec{\omega}_{FE}\|_{E(\Omega)} \tag{1.9}$$

where $\vec{\omega}_{FE}$ is the finite element solution of an *auxiliary problem*, the exact solution of which is $\vec{\omega}_{EX}$. In the auxiliary problem the domain and the mesh are the same as in the original problem but the loading is computed from the extraction function $\vec{v}$. The auxiliary solution serves theoretical purposes only: It is not necessary to know $\vec{\omega}_{EX}$ or $\vec{\omega}_{FE}$ in order to use (1.8) for computing $\Phi(\vec{u}_{FE})$. It is possible to select the extraction function $\vec{v}$ so that $\|\vec{\omega}_{EX} - \vec{\omega}_{FE}\|_{E(\Omega)} \to 0$ not slower than $\|\vec{u}_{EX} - \vec{u}_{FE}\|_{E(\Omega)} \to 0$ as $N \to \infty$ in an orderly extension process. Therefore functional values computed by extraction methods have the same order of accuracy as the strain energy or better. Functional values computed by extraction methods exhibit *superconvergence* [10,11].

In this paper we describe procedures for the extraction of the amplitude of stress singular terms associated with reentrant corners in plane elasticity. We assume that the plane elastic body is homogeneous and isotropic; loaded by boundary tractions only; in the neighborhood of the reentrant corner the boundaries are

stress free, and in (1.3) $\tilde{u}_x = 0, \quad \tilde{u}_y = 0$, however the method described herein can be generalized to other problems such as fixed-free boundary conditions; intersection of material interfaces with external boundaries; etc. We demonstrate the performance of the extraction procedures on the basis of three test problems.

2. THE EXACT SOLUTION IN THE NEIGHBORHOOD OF REENTRANT CORNERS.

In the neighborhood of reentrant corners (Fig. 2.1) we examine Airy stress functions of the form:

$$U = U(r, \theta) = r^{\lambda+1} F(\theta). \tag{2.1}$$

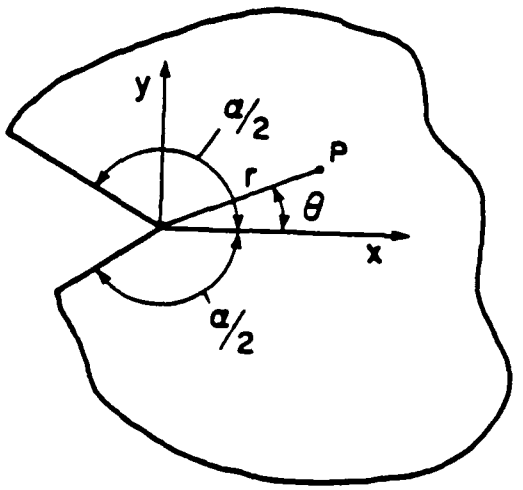

Fig. 2.1. Reentrant corner. Notation.

Because U satisfies the biharmonic equation:

$$\left(\frac{\partial^2}{\partial r^2} + \frac{1}{r}\frac{\partial}{\partial r} + \frac{1}{r^2}\frac{\partial^2}{\partial \theta^2}\right)\left(\frac{\partial^2}{\partial r^2} + \frac{1}{r}\frac{\partial}{\partial r} + \frac{1}{r^2}\frac{\partial^2}{\partial \theta^2}\right) U = 0 \tag{2.2}$$

$F(\theta)$ must satisfy:

$$F'''' + 2(\lambda^2 + 1) F'' + (\lambda^2 - 1)^2 F = 0 \tag{2.3}$$

where the primes represent differentiation with respect to θ. The general solution of (2.3) for $\lambda \neq 0$ and $\lambda \neq \pm 1$ is:

$$F(\theta) = a_1 \cos(\lambda - 1)\theta + a_2 \cos(\lambda + 1)\theta + a_3 \sin(\lambda - 1)\theta + a_4 \sin(\lambda + 1)\theta. \tag{2.4}$$

We need to determine λ and combinations of a_i $(i = 1, 2, 3, 4)$, such that the edges that meet at the reentrant corners are stress free. From the stress function U we have:

$$\sigma_\theta = \frac{\partial^2 U}{\partial r^2} = \lambda(\lambda+1) r^{\lambda-1} F(\theta) \tag{2.5a}$$

and:

$$\tau_{r\theta} = -\frac{1}{r}\frac{\partial^2 U}{\partial r \partial \theta} + \frac{1}{r^2}\frac{\partial U}{\partial \theta} = -\lambda r^{\lambda-1} F'(\theta). \tag{2.5b}$$

Along the reentrant edges (at $\theta = \pm\alpha/2$) we have $\sigma_\theta = \tau_{r\theta} = 0$. Consequently, from (2.4) and (2.5a,b), after straightforward algebraic manipulation, we have:

$$\begin{bmatrix} \cos(\lambda-1)\frac{\alpha}{2} & \cos(\lambda+1)\frac{\alpha}{2} & 0 & 0 \\ \mathrm{A}\sin(\lambda-1)\frac{\alpha}{2} & \sin(\lambda+1)\frac{\alpha}{2} & 0 & 0 \\ 0 & 0 & \sin(\lambda-1)\frac{\alpha}{2} & \sin(\lambda+1)\frac{\alpha}{2} \\ 0 & 0 & \cos(\lambda-1)\frac{\alpha}{2} & \mathrm{A}\cos(\lambda+1)\frac{\alpha}{2} \end{bmatrix} \begin{Bmatrix} a_1 \\ a_2 \\ a_3 \\ a_4 \end{Bmatrix} = 0 \tag{2.6}$$

where:

$$\mathrm{A} = \frac{1-\lambda}{1+\lambda}. \tag{2.7}$$

Note that a_1, a_2 are independent of a_3, a_4. A nontrivial solution exists only if the corresponding determinants vanish:

$$\cos(\lambda-1)\frac{\alpha}{2}\sin(\lambda+1)\frac{\alpha}{2} - \mathrm{A}\sin(\lambda-1)\frac{\alpha}{2}\cos(\lambda+1)\frac{\alpha}{2} = 0 \tag{2.8a}$$

$$\sin(\lambda-1)\frac{\alpha}{2}\cos(\lambda+1)\frac{\alpha}{2} - \mathrm{A}\cos(\lambda-1)\frac{\alpha}{2}\sin(\lambda+1)\frac{\alpha}{2} = 0 \tag{2.8b}$$

which can be simplified to:

$$\sin\lambda\alpha + \lambda\sin\alpha = 0 \tag{2.9a}$$

$$\sin\lambda\alpha - \lambda\sin\alpha = 0. \tag{2.9b}$$

See also [12-16]. Observe that if λ is a solution of (2.9a) or (2.9b), then $-\lambda$ is also a solution, however the corresponding stress field has finite strain energy only if the real part of λ is greater than zero.

Assume now that $\lambda_i^{(1)}$ $(i = 1, 2, \ldots)$ is a solution of (2.9a) and $\lambda_i^{(1)}$ is real and simple. Then, from (2.6):

$$a_1 \cos(\lambda_i^{(1)} - 1)\frac{\alpha}{2} + a_2 \cos(\lambda_i^{(1)} + 1)\frac{\alpha}{2} = 0 \tag{2.10a}$$

$$a_1 A_i^{(1)} \sin(\lambda_i^{(1)} - 1)\frac{\alpha}{2} + a_2 \cos(\lambda_i^{(1)} + 1)\frac{\alpha}{2} = 0 \tag{2.10b}$$

where: $A_i^{(1)} = \dfrac{1 - \lambda_i^{(1)}}{1 + \lambda_i^{(1)}}$. Let us define:

$$Q_i^{(1)} = \frac{a_2}{a_1} = -\frac{\cos(\lambda_i^{(1)} - 1)\frac{\alpha}{2}}{\cos(\lambda_i^{(1)} + 1)\frac{\alpha}{2}} = -\frac{A_i^{(1)} \sin(\lambda_i^{(1)} - 1)\frac{\alpha}{2}}{\sin(\lambda_i^{(1)} + 1)\frac{\alpha}{2}}. \tag{2.11}$$

With this notation (2.1) can be written as:

$$U = r^{\lambda_i^{(1)}+1}\left(\cos(\lambda_i^{(1)} - 1)\,\theta + Q_i^{(1)} \cos(\lambda_i^{(1)} + 1)\,\theta\right). \tag{2.12a}$$

Similarly, if $\lambda_i^{(2)}$ is a real, simple root of (2.9b), then the corresponding stress function is:

$$U = r^{\lambda_i^{(2)}+1}\left(\sin(\lambda_i^{(2)} - 1)\,\theta + Q_i^{(2)} \sin(\lambda_i^{(2)} + 1)\,\theta\right) \tag{2.12b}$$

where:

$$Q_i^{(2)} = -\frac{\sin(\lambda_i^{(2)} - 1)\frac{\alpha}{2}}{\sin(\lambda_i^{(2)} + 1)\frac{\alpha}{2}} = -\frac{1 - \lambda_i^{(2)}}{1 + \lambda_i^{(2)}} \frac{\cos(\lambda_i^{(2)} - 1)\frac{\alpha}{2}}{\cos(\lambda_i^{(2)} + 1)\frac{\alpha}{2}}. \tag{2.13}$$

Note that (2.12a) is symmetric with respect to θ, whereas (2.12b) is antisymmetric. From (2.12a,b) expressions from stress and displacement fields can be derived. These expressions are most conveniently obtained by first writing (2.12a,b) in terms of the complex variable z, and then using the method of Muskhelishvili [15]. The stress and displacement fields corresponding to (2.12a) are called *Mode 1* fields. The stress and displacement fields corresponding to (2.12b) are called *Mode 2* fields. Specifically, the Mode 1 displacement components, up to rigid body displacement and rotation terms, are:

$$u_{xi}^{(1)} = \frac{1}{2G} r^{\lambda_i^{(1)}} \left[\left(\kappa - Q_i^{(1)}(\lambda_i^{(1)} + 1)\right) \cos \lambda_i^{(1)}\theta - \lambda_i^{(1)} \cos(\lambda_i^{(1)} - 2)\,\theta\right] \tag{2.14a}$$

$$u_{yi}^{(1)} = \frac{1}{2G} r^{\lambda_i^{(1)}} \left[\left(\kappa + Q_i^{(1)}(\lambda_i^{(1)} + 1)\right) \sin \lambda_i^{(1)}\theta + \lambda_i^{(1)} \sin(\lambda_i^{(1)} - 2)\,\theta\right] \tag{2.14b}$$

which can be written in the form:

$$\vec{u}_i^{(1)} \equiv \{u_i^{(1)}\} = \frac{1}{2G} r^{\lambda_i^{(1)}} \{\Psi_i^{(1)}(\theta)\} \tag{2.14c}$$

In (2.14a,b,c) G is the modulus of rigidity, and κ depends only on Poisson's ratio. For plane strain:

$$\kappa = 3 - 4\nu \tag{2.15a}$$

and for plane stress:

$$\kappa = \frac{3-\nu}{1+\nu}. \tag{2.15b}$$

The Mode 1 stress tensor components are:

$$\sigma_{xi}^{(1)} = \lambda_i^{(1)} r^{\lambda_i^{(1)}-1} \left[\left(2 - Q_i^{(1)}(\lambda_i^{(1)}+1)\right)\cos(\lambda_i^{(1)}-1)\theta - (\lambda_i^{(1)}-1)\cos(\lambda_i^{(1)}-3)\theta\right] \tag{2.16a}$$

$$\sigma_{yi}^{(1)} = \lambda_i^{(1)} r^{\lambda_i^{(1)}-1} \left[\left(2 + Q_i^{(1)}(\lambda_i^{(1)}+1)\right)\cos(\lambda_i^{(1)}-1)\theta + (\lambda_i^{(1)}-1)\cos(\lambda_i^{(1)}-3)\theta\right] \tag{2.16b}$$

$$\tau_{xyi}^{(1)} = \lambda_i^{(1)} r^{\lambda_i^{(1)}-1} \left[(\lambda_i^{(1)}-1)\sin(\lambda_i^{(1)}-3)\theta + Q_i^{(1)}(\lambda_i^{(1)}+1)\sin(\lambda_i^{(1)}-1)\theta\right]. \tag{2.16c}$$

The Mode 2 displacement components, up to rigid body displacement and rotation terms, are:

$$u_{xi}^{(2)} = \frac{1}{2G} r^{\lambda_i^{(2)}} \left[\left(\kappa - Q_i^{(2)}(\lambda_i^{(2)}+1)\right)\sin\lambda_i^{(2)}\theta - \lambda_i^{(2)}\sin(\lambda_i^{(2)}-2)\theta\right] \tag{2.17a}$$

$$u_{yi}^{(2)} = -\frac{1}{2G} r^{\lambda_i^{(2)}} \left[\left(\kappa + Q_i^{(2)}(\lambda_i^{(2)}+1)\right)\cos\lambda_i^{(2)}\theta + \lambda_i^{(2)}\cos(\lambda_i^{(2)}-2)\theta\right] \tag{2.17b}$$

which can be written in the form:

$$\vec{u}_i^{(2)} \equiv \{u_i^{(2)}\} = \frac{1}{2G} r^{\lambda_i^{(2)}} \{\Psi_i^{(2)}(\theta)\}. \tag{2.17c}$$

The Mode 2 stress tensor components are:

$$\sigma_{xi}^{(2)} = \lambda_i^{(2)} r^{\lambda_i^{(2)}-1} \left[\left(2 - Q_i^{(2)}(\lambda_i^{(2)}+1)\right)\sin(\lambda_i^{(2)}-1)\theta - (\lambda_i^{(2)}-1)\sin(\lambda_i^{(2)}-3)\theta\right] \tag{2.18a}$$

$$\sigma_{yi}^{(2)} = \lambda_i^{(2)} r^{\lambda_i^{(2)}-1} \left[\left(2 + Q_i^{(2)}(\lambda_i^{(2)}+1)\right)\sin(\lambda_i^{(2)}-1)\theta + (\lambda_i^{(2)}-1)\sin(\lambda_i^{(2)}-3)\theta\right] \tag{2.18b}$$

$$\tau_{xyi}^{(2)} = -\lambda_i^{(2)} r^{\lambda_i^{(2)}-1} \left[(\lambda_i^{(2)}-1)\cos(\lambda_i^{(2)}-3)\theta + Q_i^{(2)}(\lambda_i^{(2)}+1)\cos(\lambda_i^{(2)}-1)\theta\right]. \tag{2.18c}$$

In fracture mechanics we have: $\alpha = 2\pi$. In this case (2.9a,b) are identical ($\sin 2\lambda\pi = 0$), and all roots are real and simple:

$$\lambda_i^{(1)} = \lambda_i^{(2)} = \pm\frac{1}{2},\ \pm\frac{3}{2},\ \pm 2,\ \pm\frac{5}{2}, \cdots \tag{2.19}$$

Assuming traction free crack surfaces, finite strain energy, and neglecting rigid body displacement and rotation terms, in the neighborhood of the crack tip any solution can be written in the form:

$$\{u\} = \sum_{i=1}^{\infty} \frac{A_i^{(1)}}{2G} r^{\lambda_i^{(1)}} \{\Psi_i^{(1)}(\theta)\} + \sum_{i=1}^{\infty} \frac{A_i^{(2)}}{2G} r^{\lambda_i^{(2)}} \{\Psi_i^{(2)}(\theta)\}. \tag{2.20}$$

This infinite series converges absolutely for $r < r_0$ for some $r_0 > 0$. The coefficients $A_i^{(1)}$ and $A_i^{(2)}$ are called *generalized stress intensity factors*. The coefficients $A_1^{(1)}$ and $A_1^{(2)}$ are related to the Mode 1 and Mode 2 stress intensity factors, K_I and K_{II}, as follows:

$$A_1^{(1)} = \frac{K_I}{\sqrt{2\pi}}, \qquad A_1^{(2)} = \frac{K_{II}}{\sqrt{2\pi}}. \tag{2.21}$$

Methods for the determination of the generalized stress intensity factors are discussed in the following sections.

When $\alpha \neq 2\pi$, then not all roots are real, and multiple roots (both real and complex) can exist. The cases of complex roots and multiple real roots are beyond the scope of this discussion. From the point of view of engineering analysis, the solid angles of 270, 240, 225 and 210 degrees are of the greatest importance (in addition to the 360 degrees already discussed). In these cases the smallest roots are real. Their values are shown in Table 2.1.

Table 2.1. Smallest positive roots of (9a,b) for selected solid angles (α).

α	$\lambda_1^{(1)}$	$\lambda_1^{(2)}$
360°	0.500000	0.500000
270°	0.544484	0.908529
240°	0.615731	1.148913
225°	0.673583	1.302086
210°	0.751975	1.485812

When the solid angle is greater than 257.45 degrees, then $\lambda_1^{(2)} > 1$ and the Mode 2 stress components are bounded. The Mode 1 stress components are unbounded when $\alpha > 180°$.

3. BETTI'S LAW. THE PATH INDEPENDENT INTEGRAL $I_{\Gamma^*}(\vec{u}, \vec{v})$.

We denote the strain tensor components, corresponding to the displacement field $\vec{u}(x, y)$ by $\epsilon_x^{(u)}$, $\epsilon_y^{(u)}$, $\gamma_{xy}^{(u)}$. The strain-displacement relations are:

$$\epsilon_x^{(u)} = \frac{\partial u_x}{\partial x}, \quad \epsilon_y^{(u)} = \frac{\partial u_y}{\partial y}, \quad \gamma_{xy}^{(u)} = \frac{\partial u_x}{\partial y} + \frac{\partial u_y}{\partial x}. \tag{3.1}$$

Similarly, we denote the stress tensor components corresponding to displacement field $\vec{u}(x, y)$ by $\sigma_x^{(u)}$, $\sigma_y^{(u)}$ and $\tau_{xy}^{(u)}$. The stress-strain relations are:

$$\{\sigma^{(u)}\} = [E]\{\epsilon^{(u)}\} \tag{3.2}$$

where $\{\sigma^{(u)}\} = \{\sigma_x^{(u)} \ \sigma_y^{(u)} \ \tau_{xy}^{(u)}\}^T$; $\{\epsilon^{(u)}\} = \{\epsilon_x^{(u)} \ \epsilon_y^{(u)} \ \gamma_{xy}^{(u)}\}^T$ and $[E]$ is a symmetric, positive definite matrix, called the *material stiffness matrix*. We have assumed that the initial strain is zero. We shall assume also that the body forces are zero and that $\vec{u}$ is such that the coresponding stresses, computed from (3.1) and (3.2), satisfy the equilibrium equations with zero body forces:

$$\frac{\partial \sigma_x^{(u)}}{\partial x} + \frac{\partial \tau_{xy}^{(u)}}{\partial y} = 0; \qquad \frac{\partial \tau_{xy}^{(u)}}{\partial x} + \frac{\partial \sigma_y^{(u)}}{\partial y} = 0. \tag{3.3}$$

We denote the direction cosines of the normal to the boundary of the plane elastic body at boundary point P by n_x, n_y. The traction vector components in terms of the stress components at point P are:

$$T_x^{(u)} = \sigma_x^{(u)} n_x + \tau_{xy}^{(u)} n_y \tag{3.4a}$$

$$T_y^{(u)} = \tau_{xy}^{(u)} n_x + \sigma_y^{(u)} n_y. \tag{3.4b}$$

Let $\vec{v} \equiv \{v\} = \{v_x(x, y) \ v_y(x, y)\}$ be an arbitrary displacement vector field and assume that the strain energy associated with $\vec{v}$ is finite on Ω. Assume further that tractions are specified along the entire boundary of Ω. We denote the boundary of Ω by $\partial\Omega$. In the absence of body forces, thermal loading and elastic constraints the *principle of virtual work*, states that:

$$\iint_\Omega \{\epsilon^{(v)}\}^T \{\sigma^{(u)}\} \, dx \, dy \equiv \iint_\Omega \{\epsilon^{(v)}\}^T [E] \{\epsilon^{(u)}\} \, dx \, dy = \int_{\partial\Omega} (T_x^{(u)} v_x + T_y^{u} v_y) \, ds \tag{3.5}$$

holds for any $\vec{v}$. $\vec{v}$ is called *virtual displacement*. The strain components $\{\epsilon^{(v)}\}$ are related to $\vec{v}$ by (3.1). Because $[E]$ is symmetric, (3.5) can be written as:

$$\iint_\Omega \left([E]\{\epsilon^{(v)}\}\right)^T \{\epsilon^{(u)}\}\, dx\, dy = \iint_\Omega \{\sigma^{(v)}\}^T \{\epsilon^{(u)}\}\, dx\, dy = \int_{\partial\Omega} (T_x^{(u)} v_x + T_y^{u} v_y)\, ds \qquad (3.6)$$

which is the same as:

$$\iint_\Omega \left\{\sigma_x^{(v)} \frac{\partial u_x}{\partial x} + \sigma_y^{(v)} \frac{\partial u_y}{\partial y} + \tau_{xy}^{(v)} \left(\frac{\partial u_x}{\partial y} + \frac{\partial u_y}{\partial x}\right)\right\} dx\, dy = \int_{\partial\Omega} (T_x^{(u)} v_x + T_x^{(u)} v_x)\, ds. \qquad (3.7)$$

Applying Green's lemma and using (3.4a,b) we have:

$$\int_{\partial\Omega} (T_x^{(v)} u_x + T_y^{(v)} u_y) ds - \int_{\partial\Omega} (T_x^{(u)} v_x + T_y^{(u)} v_y) ds =$$

$$\iint_\Omega \left\{\left(\frac{\partial \sigma_x^{(v)}}{\partial x} + \frac{\partial \tau_{xy}^{(v)}}{\partial y}\right) u_x + \left(\frac{\partial \tau_{xy}^{(v)}}{\partial x} + \frac{\partial \sigma_y^{(v)}}{\partial y}\right) u_y\right\} dx\, dy. \qquad (3.8)$$

When the stresses corresponding to both $\vec{u}$ and $\vec{v}$ satisfy the equilibrium equations with the body forces equal to zero, that is (3.3) then we have *Betti's law*:

$$\int_{\partial\Omega} (T_x^{(v)} u_x + T_y^{(v)} u_y)\, ds = \int_{\partial\Omega} (T_x^{(u)} v_x + T_y^{(u)} v_y)\, ds \qquad (3.9a)$$

where the integration is *countreclockwise* around Ω. We denote the normal and tangential traction vector components respectively by T_n and T_t and the normal and tangential displacement vector components by u_n and u_t. Because: $T_x^{(v)} u_x + T_y^{(v)} u_y = T_n^{(v)} u_n + T_t^{(v)} u_t$, etc., Betti's law can be also written in the following form:

$$\int_{\partial\Omega} (T_n^{(v)} u_n + T_t^{(v)} u_t)\, ds = \int_{\partial\Omega} (T_n^{(u)} v_n + T_t^{(u)} v_t)\, ds. \qquad (3.9b)$$

Let us now consider a subdomain of Ω, denoted by Ω^*, in the neighborhood of the reentrant corner. Ω^* is bounded by two continuous curves, Γ_1^* and Γ_2^*, and the reentrant edges, as shown in Fig. 3.1. Let $\{u\}$ and $\{v\}$ be two displacement fields, both satisfying the equilibrium equations with body forces and initial strains equal to zero, and the stress free boundary conditions along the reentrant edges ($\sigma_\theta = \tau_{r\theta} = 0$ at $\theta = \pm\alpha/2$). Then, according to Betti's law:

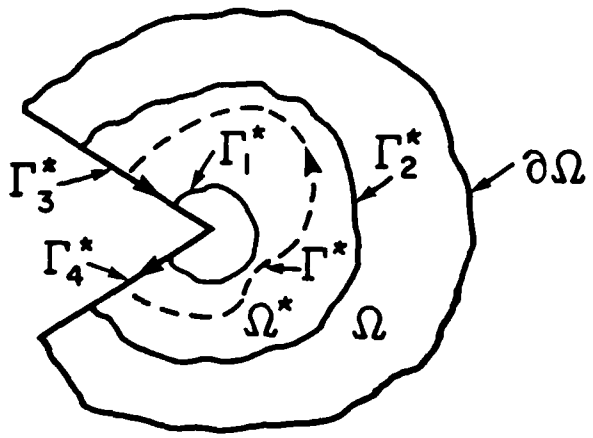

Fig. 3.1. The subdomain Ω^*.

$$\int_{\Gamma_1^*}(T_n^{(v)}u_n + T_t^{(v)}u_t)ds + \int_{\Gamma_2^*}(T_n^{(v)}u_n + T_t^{(v)}u_t)ds =$$

$$\int_{\Gamma_1^*}(T_n^{(u)}v_n + T_t^{(u)}v_t)ds + \int_{\Gamma_2^*}(T_n^{(u)}v_n + T_t^{(u)}v_t)ds. \tag{3.10}$$

We integrate around Ω^* in the counterclockwise direction. Therefore integration along Γ_2^* is in the counterclockwise direction, while integration along Γ_1^* is in the clockwise direction with respect to the reentrant corner. Let us reverse the sense of the direction of the integral along Γ_1^* so that both contour integrals are in the counterclockwise direction with respect to the reentrant corner. We will use the symbol $\tilde{\Gamma}_1^*$ to indicate integration along Γ_1^* in the counterclockwise direction with respect to the reentrant corner. In this case we have:

$$\int_{\tilde{\Gamma}_1^*}(T_n^{(u)}v_n + T_t^{(u)}v_t)ds - \int_{\tilde{\Gamma}_1^*}(T_n^{(v)}u_n + T_t^{(v)}u_t)ds =$$

$$\int_{\Gamma_2^*}(T_n^{(u)}v_n + T_t^{(u)}v_t)ds - \int_{\Gamma_2^*}(T_n^{(v)}u_n + T_t^{(v)}u_t)ds. \tag{3.11}$$

Therefore, the integral:

$$I_{\Gamma^*}(\vec{u},\vec{v}) = \int_{\Gamma^*}(T_n^{(u)}v_n + T_t^{(u)}v_t)ds - \int_{\Gamma^*}(T_n^{(v)}u_n + T_t^{(v)}u_t)ds \tag{3.12}$$

is independent of the path Γ^*. Of course, Γ^* must begin on the reentrant edge and terminate on the other reentrant edge, as shown in Fig. 3.1, and the integration must be counterclockwise with respect to the reentrant corner.

When the stresses corresponding to $\{v\}$ do not satisfy the equilibrium equations and the stress free boundary conditions along the reentrant edges, then instead of (3.11) we have:

$$\int_{\tilde{\Gamma}_1^*}(T_n^{(u)}v_n + T_t^{(u)}v_t)ds - \int_{\tilde{\Gamma}_1^*}(T_n^{(v)}u_n + T_t^{(v)}u_t)ds =$$

$$\int_{\Gamma_2^*}(T_n^{(u)}v_n + T_t^{(u)}v_t)ds - \int_{\Gamma_2^*}(T_n^{(v)}u_n + T_t^{(v)}u_t)ds - \int_{\Gamma_3^*}(T_n^{(v)}u_n + T_t^{(v)}u_t)ds -$$

$$\int_{\Gamma_4^*}(T_n^{(v)}u_n + T_t^{(v)}u_t)ds + \iint_{\Omega^*}\left\{\left(\frac{\partial\sigma_x^{(v)}}{\partial x} + \frac{\partial\tau_{xy}^{(v)}}{\partial y}\right)u_x + \left(\frac{\partial\tau_{xy}^{(v)}}{\partial x} + \frac{\partial\sigma_y^{(v)}}{\partial y}\right)u_y\right\}dx\,dy. \quad (3.13)$$

The sense of integration along Γ_3 and Γ_4 is shown in Fig. 3.1.

4. EXTRACTION OF STRESS INTENSITY FACTORS.

In the following we consider only real and simple roots of (2.9a) and (2.9b). This is the case in linear elastic fracture mechanics. We present two algorithmic procedures for the computation of coefficients $A_i^{(m)}$ $(i = 1, 2, \ldots;\ m = 1, 2)$ in (2.20). The restriction to real and simple root is not essential however, and all coefficients of asymptotic expansions, similar to (2.20), can be determined by the methods described in this section.

4.1. The contour integral method.

Let Γ_ρ be a circle of radius ρ centered on the crack tip, and assume that ρ is sufficiently close to the crack tip so that the exact solution $\{u_{EX}\}$ is represented by (2.20) on Γ_ρ. The traction vector, corresponding to $\{u_{EX}\}$, can be written as:

$$\{T_i^{(u_{EX})}\} = \sum_{i=1}^{\infty}\sum_{m=1}^{2} A_i^{(m)}\lambda_i^{(m)}r^{\lambda_i^{(m)}-1}\{\Upsilon_i^{(m)}(\theta)\}. \quad (4.1)$$

where $\lambda_i^{(1)} > 0$ is a real and simple root of (2.9a) and $\lambda_i^{(2)} > 0$ is a real and simple root of (2.9b).

Let $-\lambda_j^{(n)}$ be a *negative* root of (2.9a) or (2.9b), and denote the corresponding displacement function by $\{v_{-j}^{(n)}\}$:

$$\{v_{-j}^{(n)}\} = A_{-j}^{(n)} r^{-\lambda_j^{(n)}} \{\Psi_{-j}^{(n)}(\theta)\} \tag{4.2}$$

where $A_{-j}^{(n)}$ is a constant, to be determined later. Note that $\{v_{-j}^{(n)}\}$ does not have finite strain energy on Ω and, therefore, is not an admissible displacement function on Ω. It is admissible, however, on Ω^* (Fig. 3.1). The traction vector on Γ_1^*, corresponding to $\{v_{-j}^{(n)}\}$, is:

$$\{T_{-j}^{(v_{-j}^{(n)})}\} = -A_{-j}^{(n)} \lambda_j^{(n)} r^{-\lambda_j^{(n)}-1} \{\Upsilon_{-j}^{(n)}(\theta)\}. \tag{4.3}$$

We now show that:

$$I_{\Gamma_\rho}(\vec{u}_{EX}, \vec{v}_{-j}^{(n)}) = \begin{cases} A_{-i}^{(m)} A_i^{(m)} c_i^{(m)}(\alpha) & \text{if } i = j \text{ and } m = n \\ 0 & \text{otherwise} \end{cases} \tag{4.4}$$

where Γ_ρ is a circular arc of radius ρ centered on the reentrant corner. $c_i^{(m)}(\alpha)$ depends only on $\lambda_i^{(m)}$. The proof is straightforward. By direct evaluation from the absolutely convergent series (2.20), we have:

$$I_{\Gamma_\rho}(\vec{u}_{EX}, \vec{v}_{-j}^{(n)}) = A_{-j}^{(n)} \sum_{i=1}^{\infty} \sum_{m=1}^{2} A_i^{(m)} \rho^{\lambda_i^{(m)} - \lambda_j^{(n)}} C_{i,-j}^{(m,n)}, \quad (n = 1, 2) \tag{4.5a}$$

where:

$$C_{i,-j}^{(m,n)} = \frac{1}{2G} \int_{-\alpha/2}^{+\alpha/2} \left(\{\Psi_{-j}^{(n)}(\theta)\}^T \{\Upsilon_i^{(m)}(\theta)\} + \{\Psi_i^{(m)}(\theta)\}^T \{\Upsilon_{-j}^{(n)}(\theta)\} \right) d\theta. \tag{4.5b}$$

Because $I_{\Gamma_\rho}(\vec{u}_{EX}, \vec{v}_{-j}^{(n)})$ is independent of Γ_ρ, it is independent of ρ. If $\lambda_i^{(m)} \neq \lambda_j^{(n)}$, then this is possible only if the integral expression (4.5b) is zero. The other possibility is that $\lambda_i^{(m)} = \lambda_j^{(n)}$, but $n \neq m$. In this case, however, the integrand in (4.5b) is the sum of the dot products of symmetric and antisymmetric vector functions

therefore the integral is zero. Denoting: $c_i^{(m)}(\alpha) = C_{i,-i}^{(m,m)}$, we have (4.4) and letting $A_{-i}^{(m)} = 1/c_i^{(m)}(\alpha)$, we have from (3.10):

$$A_i^{(m)} = \int_{\Gamma_2^*} \left(\{v_{-i}^{(m)}\}^T \{T^{(u_{BX})}\} \right) ds - \int_{\Gamma_2^*} \left(\{u_{EX}\}^T \{T^{(v_{-i}^{(m)})}\} \right) ds \tag{4.6}$$

where Γ_2^* is, of course, arbitrary. The function $\{v_{-i}^{(m)}\}$ is an *extraction function* for $A_i^{(m)}$. Of course, we do not know $\{u_{EX}\}$ and $\{T^{(u_{BX})}\}$. We therefore substitute $\{u_{FE}\}$ and $\{T^{(u_{FB})}\}$ in (4.6) for $\{u_{EX}\}$ and $\{T^{(u_{BX})}\}$ to obtain an approximation to $A_i^{(m)}$. If Γ_2^* includes an external boundary where the imposed tractions are known, then the imposed tractions can be used in (4.6). Implementation would pose some difficulties, however, and computational experience has shown that the use of $\{T^{(u_{FB})}\}$ instead of the imposed tractions generally yields satisfactory results. Examples are presented in Section 5.

4.2. The cutoff function method.

Let us now assume that both contours Γ_1^* and Γ_2^* are circular arcs with radii ρ_1 and ρ_2, respectively, $\rho_1 < \rho_2$. We define the following extraction function for $A_i^{(m)}$:

$$\{w_{-i}^{(m)}\} = \phi(r)\{v_{-i}^{(m)}\} \tag{4.7}$$

where $\{v_{-i}^{(m)}\}$ is defined by (4.2), and $\phi(r)$ is called the *cutoff function* and is defined by:

$$\phi(r) = \begin{cases} 1 & r \le \rho_1 \\ 1 - 3\left(\dfrac{r-\rho_1}{\rho_2-\rho_1}\right)^2 + 2\left(\dfrac{r-\rho_1}{\rho_2-\rho_1}\right)^3 & \rho_1 < r < \rho_2 \\ 0 & r \ge \rho_2. \end{cases} \tag{4.8}$$

In this case the extraction function satisfies neither the stress free boundary conditions on the reentrant edges nor the equilibrium equations. Therefore, (3.13) must be used for the computation of $A_i^{(m)}$, instead of (3.11). Specifically, if we select $A_{-i}^{(m)}$ as before, i.e: $A_{-i}^{(m)} = 1/c_i^{(m)}(\alpha)$, where $c_i^{(m)}(\alpha)$ is computed from (4.5b) with $\{v_{-i}^{(m)}\}$ replaced by $\{w_{-i}^{(m)}\}$, we have:

$$A_i^{(m)} = \int_{\Gamma_2^*} (T_n^{(w_{-i}^{(m)})} u_n + T_t^{(w_{-i}^{(m)})} u_t) ds - \int_{\Gamma_2^*} (T_n^{(w_{-i}^{(m)})} u_n + T_t^{(w_{-i}^{(m)})} u_t) ds$$

$$+\iint_{\Omega^*}\left\{\left(\frac{\partial\sigma_x^{(w_{-1}^{(m)})}}{\partial x}+\frac{\partial\tau_{xy}^{(w_{-1}^{(m)})}}{\partial y}\right)u_x+\left(\frac{\partial\tau_{xy}^{(w_{-1}^{(m)})}}{\partial x}+\frac{\partial\sigma_y^{(w_{-1}^{(m)})}}{\partial y}\right)u_y\right\}dx\,dy. \qquad (4.9)$$

The contour integrals must be evaluated along the reentrant edges in the counterclockwise direction with respect to Ω^* (see Fig. 3.1). The advantage of the cutoff function method is that stresses and tractions corresponding to $\{u_{FE}\}$ do not have to be considered. For this reason the cutoff function method is more accurate than the contour integral method.

5. EXAMPLES.

The contour integral and cutoff function methods can be implemented in any finite element computer program. However, the error in the computed data is closely related to the error in energy norm and therefore the design of the finite element space $S^p(\Omega,\Delta,Q)$ [10,11]. Also, the cutoff function method requires the use of smooth mapping techniques. The following example problems were solved by means of a new computer program, called *PROBE*. *PROBE* implements the *p-version* of the finite element method, that is sequences of finite element spaces $S^p(\Omega,\Delta,Q)$ can be conveniently created by letting $p = 1,2,\ldots 8$ while keeping the mesh Δ and the mappings Q fixed. Of course, the mesh and the mappings can be changed also. The mapping of finite elements is by the *linear blending function method.* Curved boundaries, such as circles, and other conical sections are represented exactly in the computation of stiffness matrices and load vectors. *PROBE* also permits specification of loading by *FORTRAN*-like expressions, hence boundary tractions specified herein were represented exactly in the load vector computations. Twelve Gauss points used in the computation of load vectors independently of the polynomial degree. In the case of extraction methods 12 Gauss points are used for evaluating the contour integrals in and 144 Gauss points are used for evaluating the area integrals, independently of the polynomial degree. Additional details concerning *PROBE* are available in [17].

Other examples of the application of extraction methods, based on experimental (research) implementations, are available in [18,19].

5.1. L-shaped plane elastic body.

We consider the L-shaped plane elastic body of thickness t, shown in Fig. 5.1, loaded by tractions corresponding to the first symmetric and antisymmetric

eigenfunctions of the asymptotic expansion of $\vec{u}_{EX}$ about the reentrant corner. This example is representative of plate and shell intersections and reentrant corner problems in general.

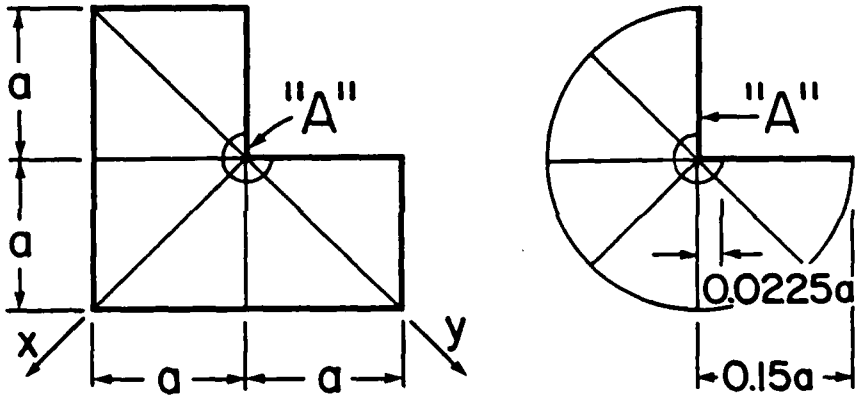

Fig. 5.1. L-shaped plane elastic body. Mesh design (18 elements).

We select $\nu = 0.3$ and assume *plane strain* conditions. Therefore $\kappa = 1.8$; $\lambda_1^{(1)} = 0.54448374$; $Q_1^{(1)} = 0.543075579$; $\lambda_1^{(2)} = 0.90852919$; $Q_1^{(2)} = -0.218923236$ [see (2.15a), (2.9a,b), (2.11) and (2.13)]. We superimpose the tractions corresponding to the stress components (2.16) and (2.18) along the boundaries of the L-shaped plane elastic body with the stress intensity factors selected so that $A_1^{(1)} = A$, (A is arbitrary) and:

$$A_1^{(2)} = 2\,A\,a^{\lambda_1^{(1)} - \lambda_1^{(2)}} \tag{5.1}$$

where a is the dimension shown in Fig. 5.1. In this way the exact strain energy can be computed:

$$U(\vec{u}_{EX}) = 6.77776914\,\frac{(Aa^{\lambda_1^{(1)}})^2 t}{E} \tag{5.2}$$

where E is the modulus of elasticity.

In the contour integral method (CIM) the integration was performed along the circle of radius $0.15\,a$ and the finite element solutions were computed from the elements *inside* the circle.

The number of degrees of freedom, the computed values of the normalized strain energy and the normalized stress intensity factors, defined by:

$$\tilde{A}_1^{(1)} \stackrel{\text{def}}{=} \frac{(A_1^{(1)})_{FE}}{A} \qquad \tilde{A}_1^{(2)} \stackrel{\text{def}}{=} \frac{(A_1^{(2)})_{FE}}{A\,a^{\lambda_1^{(1)} - \lambda_1^{(2)}}} \tag{5.3}$$

are listed in Table 5.1. Of course, $\tilde{A}_1^{(1)}$ has to converge to 1 and, in view of (5.3), $\tilde{A}_1^{(2)}$ has to converge to 2.

Table 5.1. L-shaped domain. Strain energy and the normalized stress intensity factors $\tilde{A}_1^{(1)}$, $\tilde{A}_1^{(2)}$ computed by the contour integral method (CIM) and the cutoff function method (CFM).

p	N	$\frac{U(\tilde{u}_{FE})E}{(A a^{\lambda_1^{(1)}})^2 t}$	$\tilde{A}_1^{(1)}$ (CIM)	$\tilde{A}_1^{(1)}$ (CFM)	$\tilde{A}_1^{(2)}$ (CIM)	$\tilde{A}_1^{(2)}$ (CFM)
1	41	6.42072796	1.18041	0.95268	2.43474	2.29075
2	119	6.74137580	0.95418	1.02177	2.01352	2.08422
3	209	6.77029847	1.02786	1.00250	2.02597	2.02239
4	335	6.77575144	0.99014	1.00073	1.99801	2.00437
5	497	6.77683967	1.00444	0.99991	2.00265	2.00097
6	695	6.77719530	0.99784	0.99985	1.99939	2.00022
7	929	6.77736281	1.00074	0.99987	2.00036	2.00005
8	1199	6.77746228	0.99952	0.99990	1.99988	2.00001
∞	∞	6.77776914	1.00000	1.00000	2.00000	2.0000

We see from Table 5.1 that the stress intensity factors computed by both methods converge strongly and obviously, although not monotonically. Greater accuracy and more nearly monotonic convergence is exhibited by the cutoff function method than the contour integral method, nevertheless both methods yield solutions which are within the range of precision normally needed in engineering computations at $p = 2$ or $p = 3$.

We have plotted the relative error in strain energy and the absolute value of the relative error in the Mode 1 and Mode 2 stress intensity factors computed by the cutoff function method against the number of degrees of freedom on log-log scale in Fig. 5.2a and on a semilog scale (the logarithms of the relative errors vs. $N^{1/3}$) in Fig. 5.2b. These choices of scale are motivated by estimates (1.7a) and (1.7b), respectively. These diagrams indicate that the error in strain energy behaves differently in the range of low p values than in the range of high p values. In the range of low p values it curves downward in Fig. 5.2a and very nearly follows a straight line path in Fig. 5.2b, suggesting that estimate (1.7b) holds. We will refer to this as Phase 1. In the range of high p values it follows a straight line path in Fig. 5.2a but has a positive, decreasing curvature in Fig. 5.2b. We will

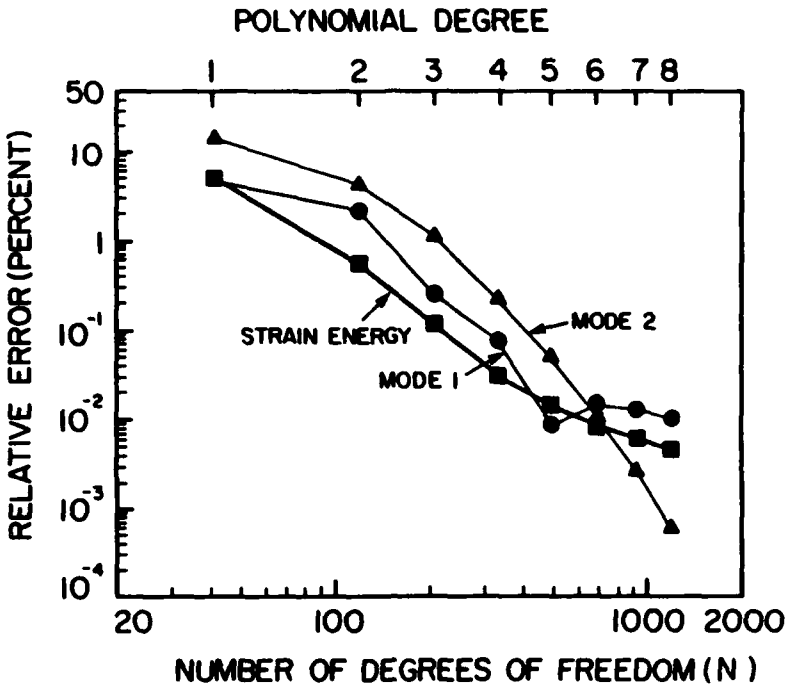

Fig. 5.2a. Convergence of the strain energy and the Mode 1 and Mode 2 stress intensity factors computed by the cutoff function method. Log-log scale.

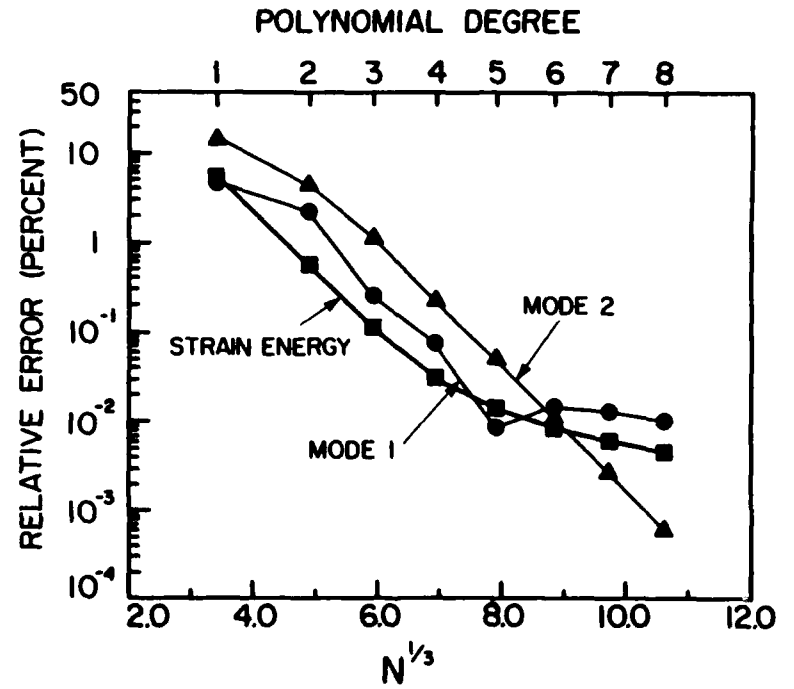

Fig. 5.2b. Convergence of the strain energy and the Mode 1 and Mode 2 stress intensity factors computed by the cutoff function method. Semilog scale.

refer to this as Phase 2. Transition from Phase 1 to Phase 2 occurs at about $p = 4$. Phase 2 is the asymptotic convergence for p-extensions: Estimate (1.7a) holds with $\beta = 2\,\lambda_1^{(1)}$, in this case $\beta = 1.089$. Phase 1 is characteristic for h-p extensions.

Obviously, the rate of decrease of the error is much faster in Phase 1 than in Phase 2. We can extend Phase 1 by refining the mesh further so that the elements are graded in geometric progression toward the reentrant corner with a common factor of about 0.15. Thus the next layer of elements around the reentrant corner would have the size of $0.15^3 a$. In general, the mesh should be designed so that the desired level of precision is achieved in Phase 1. In this example the relative errors are less than one percent in Phase 1, therefore no further refinement was necessary.

The convergence path of the Mode 1 stress intensity factor follows closely that of the strain energy, whereas the the Mode 2 stress intensity factor converges faster. This point is discussed in [10,11].

5.2. Edge cracked panel problem 1.

Let us now consider the edge cracked panel shown in Fig. 5.3. We assume *plane strain* conditions and Poisson's ratio of 0.3. In this case $\lambda_1^{(1)} = \lambda_1^{(2)} = 1/2$, therefore $Q_1^{(1)} = -1/3$ and $Q_1^{(2)} = 1$. Once again we denote the thickness of the panel by t. We apply tractions along sides A, B, C, D, E, F of the edge cracked panel shown in Fig. 5.3 that exactly correspond to the stresses of Mode 1 and Mode 2 stress fields. in this case, using appropriate trigonometric identities, (2.16a,b,c) and (2.18a,b,c) can be written in the following form (see, for example, [20]):

$$\sigma_{x1}^{(1)} = \frac{K_I}{\sqrt{2\pi r}} \cos\frac{\theta}{2}\left(1 - \sin\frac{\theta}{2}\sin\frac{3\theta}{2}\right) \tag{5.4a}$$

$$\sigma_{y1}^{(1)} = \frac{K_I}{\sqrt{2\pi r}} \cos\frac{\theta}{2}\left(1 + \sin\frac{\theta}{2}\sin\frac{3\theta}{2}\right) \tag{5.4b}$$

$$\tau_{xy1}^{(1)} = \frac{K_I}{\sqrt{2\pi r}} \sin\frac{\theta}{2}\cos\frac{\theta}{2}\cos\frac{3\theta}{2} \tag{5.4c}$$

where $-\pi \le \theta \le \pi$. The Mode 2 stress components are:

$$\sigma_{x1}^{(2)} = -\frac{K_{II}}{\sqrt{2\pi r}} \sin\frac{\theta}{2}\left(2 + \cos\frac{\theta}{2}\cos\frac{3\theta}{2}\right) \tag{5.5a}$$

$$\sigma_{y1}^{(2)} = \frac{K_{II}}{\sqrt{2\pi r}} \sin\frac{\theta}{2}\cos\frac{\theta}{2}\cos\frac{3\theta}{2} \tag{5.5b}$$

$$\tau_{xy1}^{(2)} = \frac{K_{II}}{\sqrt{2\pi r}} \cos\frac{\theta}{2}\left(1 - \sin\frac{\theta}{2}\sin\frac{3\theta}{2}\right). \tag{5.5c}$$

The generalized stress intensity factors $A_1^{(1)}$ and $A_1^{(2)}$, are related to the stress intensity factors by (2.21). We select $K_I = K_{II} = \sqrt{2\pi}\,A$ (A is arbitrary) and define the normalized stress intensity factors $\tilde{A}_1^{(1)}$ and $\tilde{A}_1^{(2)}$ as follows:

$$\tilde{A}_1^{(1)} \stackrel{\text{def}}{=} \frac{(A_1^{(1)})_{FE}}{A} \qquad \tilde{A}_1^{(2)} \stackrel{\text{def}}{=} \frac{(A_1^{(2)})_{FE}}{A} \tag{5.6}$$

In this way the computed values of both $\tilde{A}_1^{(1)}$ and $\tilde{A}_1^{(2)}$ converge to 1 and therefore it is easy to monitor convergence of the stress intensity factors. The exact strain energy is known:

$$U(\vec{u}_{EX}) = 10.5412281\,\frac{A^2\,a\,t}{E} \tag{5.7}$$

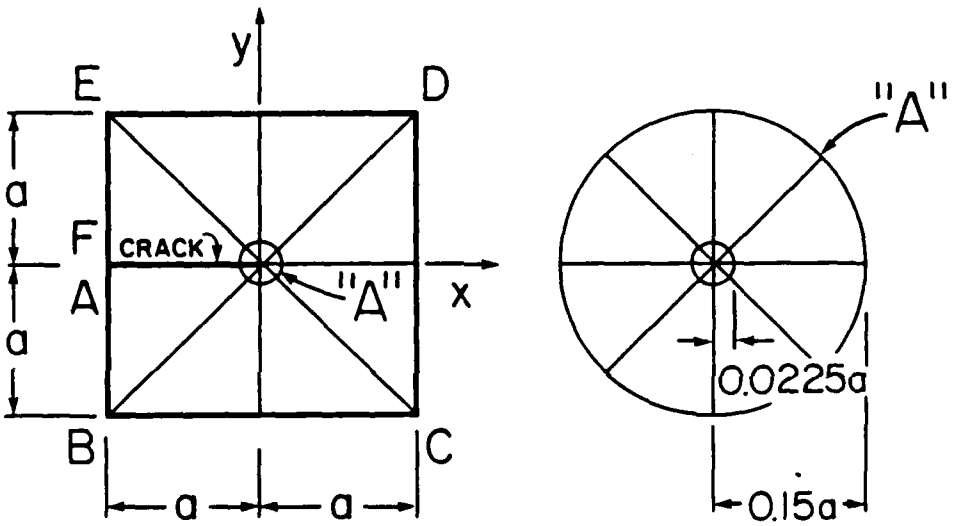

Fig. 5.3. Edge cracked panel problem 1. Mesh design (24 elements).

The number of degrees of freedom, the computed values of the normalized strain energy and the normalized stress intensity factors defined in (5.6) are shown in Table 5.2.

We see from Table 5.2 that again the cutoff function method is somewhat more accurate than the the contour integral method. In the case of the cutoff function method the relative error falls below 1 percent at p=3; in the case of the contour integral method the relative error drops below 1 percent at p=5.

The relative errors in strain energy and the absolute value of the relative error in the Mode 1 and Mode 2 stress intensity factors, computed by the cutoff

Table 5.2. Values of $\tilde{A}_1^{(1)}$ and $\tilde{A}_1^{(2)}$ computed by the contour integral and cutoff function methods.

p	N	$\frac{U(\vec{u}_{FE})E}{A^2 at}$	$\tilde{A}_1^{(1)}$ (CIM)	$\tilde{A}_1^{(1)}$ (CFM)	$\tilde{A}_1^{(2)}$ (CIM)	$\tilde{A}_1^{(2)}$ (CFM)
1	53	9.5959919	1.16972	0.91371	1.31197	1.00163
2	155	10.4114292	0.92515	1.02702	0.92840	1.04058
3	273	10.5085887	1.03787	1.00277	1.04413	1.00637
4	439	10.5302827	0.98483	1.00025	0.98360	1.00134
5	653	10.5354556	1.00609	0.99943	1.00737	0.99992
6	915	10.5374132	0.99650	0.99944	0.99639	0.99978
7	1225	10.5384252	1.00083	0.99954	1.00125	0.99978
8	1583	10.5390566	0.99907	0.99964	0.99917	0.99982
∞	∞	10.5412281	1.00000	1.00000	1.00000	1.00000

function method, are plotted against the number of degrees of freedom on log-log scale in Fig. 5.4. The inverted S-curve, typical of p-convergence when strongly graded meshes are used, is clearly visible. The stress intensity factors converge at about the same rate as the strain energy. The curves appear to enter Phase 2 at $p = 7$ or $p = 8$. The results are in agreement with the theoretical estimate given in [10].

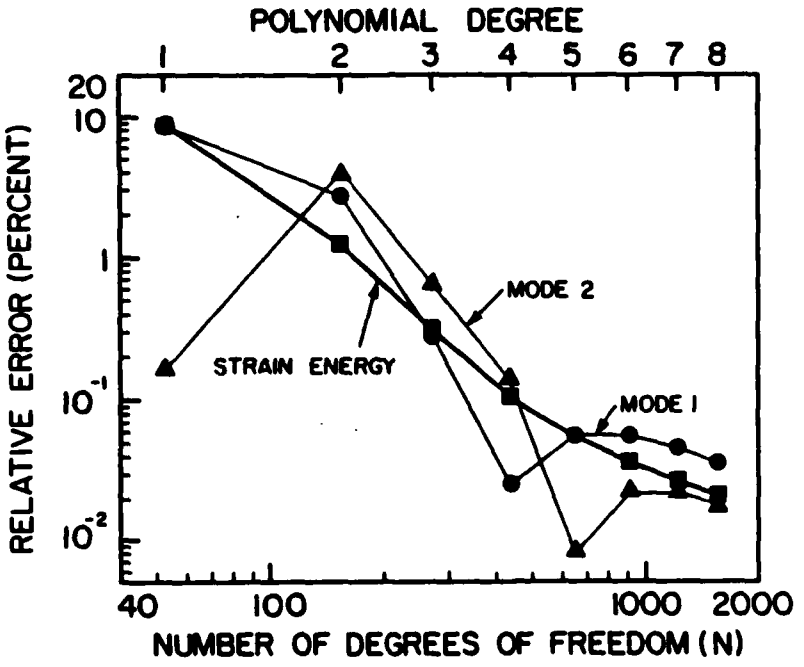

Fig. 5.4. Convergence of the strain energy and the Mode 1 and Mode 2 stress intensity factors computed by the cutoff function method.

Finally, let us examine the vector length of stress intensity factors which

can be computed by the energy release rate method also known as the stiffness derivative method. Because we have selected for this test problem $K_I = K_{II} = \sqrt{2\pi}A$, we define the computed values of of the normalized vector length of the stress intensity factors as follows:

$$\tilde{K} \stackrel{\text{def}}{=} \frac{1}{2\sqrt{\pi}A}\left(\sqrt{K_I^2 + K_{II}^2}\right)_{FE} \tag{5.8}$$

In this way $\tilde{K}$ must converge to 1. The normalized vector length of stress intensity factors, computed by the energy release rate method, the contour integral method and the cutoff function method, is shown in Table 5.3. The three methods are seen to converge strongly. Again, the performance of the cutoff function method is seen to be the strongest.

Table 5.3 Normalized vector length of stress intensity factors ($\tilde{K}$) computed by the energy release rate method (ERM), the contour integral method (CIM) and the cutoff function method (CFM).

p	ERM	CIM	CFM
1	1.06576	1.24288	0.95868
2	1.02237	0.92678	1.03382
3	0.99926	1.04100	1.00457
4	0.99663	0.98421	1.00080
5	0.99658	1.00673	0.99967
6	0.99733	0.99644	0.99961
7	0.99795	1.00104	0.99966
8	0.99840	0.99912	0.99973
∞	1.00000	1.00000	1.00000

5.3. Edge cracked panel problem 2.

The two problems just discussed were constructed so that only the first symmetric and antisymmetric terms of the asymptotic expansions were nonzero. This permitted us to examine the performance of the contour integral and cutoff function methods. In practical problems no such restrictions apply and the exact solution is not known. The following test problem is more nearly representative of practical problems.

The problem definition and mesh design are shown in Fig. 5.5. *Plane stress* condition and Poisson's ratio of 0.3 are assumed. Solutions were obtained by

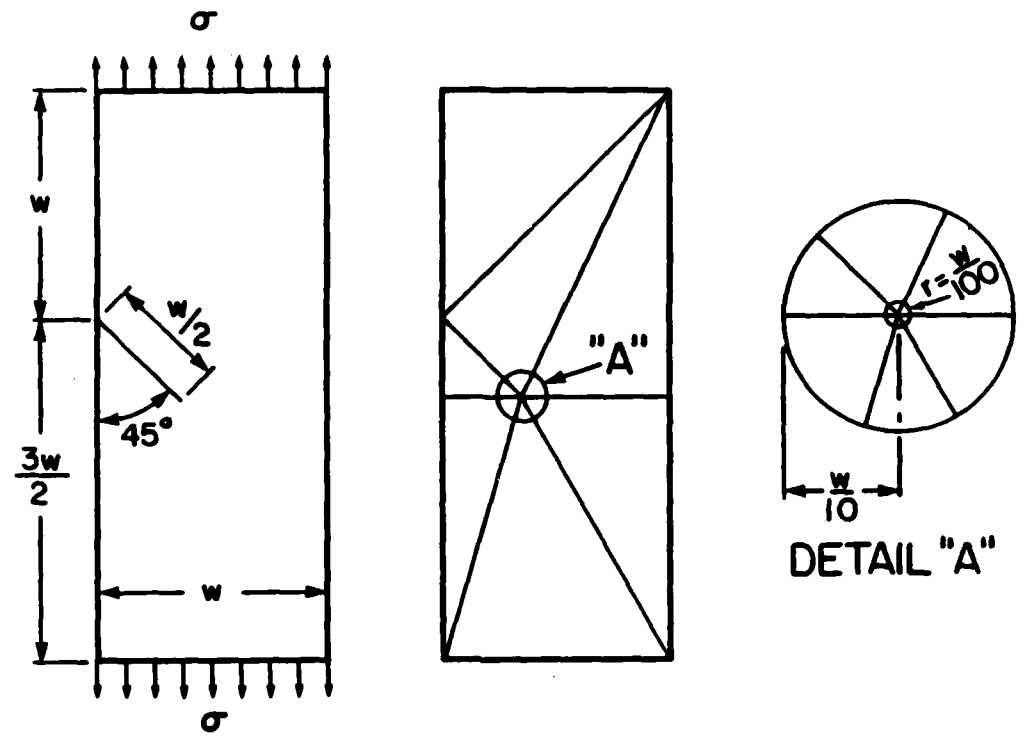

Fig. 5.5. Edge cracked panel problem 2. Mesh design.

the virtual crack extension method, the contour integral method and the cutoff function method. We normalize the stress intensity factors K_I, K_{II} and their vector length K as follows:

$$\tilde{K}_I \stackrel{\text{def}}{=} \frac{K_I}{\sigma\sqrt{2\pi\, w}}; \quad \tilde{K}_{II} \stackrel{\text{def}}{=} \frac{K_{II}}{\sigma\sqrt{2\pi\, w}}; \quad \tilde{K} \stackrel{\text{def}}{=} \frac{\sqrt{K_I^2 + K_{II}^2}}{\sigma\sqrt{w}}. \tag{5.9}$$

The results are shown in Tables 5.4 and 5.5. This problem was solved by Sha and Yang using the virtual crack extension method [21] and by Andersson [22] using a technique similar to that proposed by Rybicki and Kanninen [23]. The results presented herein agree very closely with the results given in [21,22].

The results indicate that the computed values converge strongly. Our ability to go beyond the level of precision we actually need at a small marginal cost is very important from the point of quality control: There are no other means for ensuring the quality of computed data in practical computations where the exact solution is generally not known.

Finally we note that the contour integral and cutoff function methods require substantially fewer CPU cycles than the virtual crack extension method. In the

Table 5.4. Solution by the energy release rate method.
Normalized strain energy and vector length of stress intensity factors.

p	N	$\frac{U(\vec{u}_{FE})E}{\sigma^2 w}$	$\tilde{K}$
1	43	1.4849947	1.439
2	125	1.6162227	1.605
3	221	1.6593481	1.587
4	355	1.6940543	1.656
5	527	1.7010749	1.666
6	737	1.7030296	1.671
7	985	1.7035357	1.673
8	1271	1.7037223	1.674

Table 5.5. Solutions by the contour integral and cutoff function methods.
Normalized stress intensity factors and their vector length.

p	N	$\tilde{K}_I$ (CIM)	$\tilde{K}_I$ (CFM)	$\tilde{K}_{II}$ (CIM)	$\tilde{K}_{II}$ (CFM)	$\tilde{K}$ (CIM)	$\tilde{K}$ (CFM)
1	43	0.54127	0.42259	−0.37480	−0.29005	1.650	1.285
2	125	0.49708	0.55588	−0.25578	−0.28292	1.401	1.563
3	221	0.58909	0.56161	−0.28951	−0.27074	1.645	1.563
4	355	0.57864	0.59232	−0.28319	−0.29022	1.615	1.653
5	527	0.60558	0.59825	−0.29398	−0.29012	1.687	1.667
6	737	0.59672	0.60043	−0.28897	−0.29097	1.662	1.672
7	985	0.60313	0.60119	−0.29196	−0.29091	1.680	1.674
8	1271	0.60032	0.60132	−0.29042	−0.29095	1.672	1.674

case of this example five elements have vertices on the crack tip. Therefore, using the central difference formula for evaluting the rate of change of the potential energy with respect to the crack length, we needed to recompute the stiffness matrices of five elements twice. At $p = 8$ the virtual crack extension method required 13.5 (resp. 10.5) times the CPU time required by the contour integral (resp. cutoff function) method. Also, the contour integral and cutoff function methods yield the Mode 1 and Mode 2 stress intensity factors separately whereas the virtual crack extension method does not.

6. SUMMARY AND CONCLUSIONS.

We have described two methods for the computation of the amplitudes of the first symmetric and antisymmetric terms of the asymptotic expansions of the solution at reentrant corners with stress free boundaries. This class of problems is very important from the practical point of view because it includes the problems of linear elastic fracture mechanics and in many cases the sites of failure initiation are reentrant corners.

The limiting assumptions of this paper were adopted in order to keep the presentation as simple as possible: The extraction methods described herein are not intrinsically limited to the class of problems considered here, but implementation for the general case is somewhat more difficult. For example, we have considered real and simple roots of (2.9a,b) only. If the solid angle is 360° then all roots are real and simple and the procedures presented herein can be applied directly to computing any number of coefficients of the asymptotic expansion. If the solid angle is arbitrary and the amplitudes of several terms of the asymptotic expansion are of interest then the implementation must account for multiple real roots and complex roots as well. Complications arise also when the material properties change, such as along the edge of a composite panel. In such cases determination of the eigenvalues and eigenfunctions is more difficult than in the case discussed here. (See, for example, [24].) These difficulties notwithstanding, implementation of procedures for the computation of the asymptotic expansion of stress singular terms is feasible. We have demonstrated that the amplitudes computed by the contour integral and cutoff function methods converge to their true values at about the same rate as the strain energy, or faster. Thus the amplitudes can be computed accurately and inexpensively by these methods.

The accuracy depends on the design of the finite element mesh and the choice of polynomial degree. In general the mesh should be designed and the polynomial degree chosen so that the desired level of accuracy is reached just before transition occurs from Phase 1 to Phase 2 in the p-extension process. Procedures for correct mesh design and proper selection of p are discussed in [7,25].

P-extensions can be implemented, and in fact have been implemented in *PROBE*, so that once the solution for $p = p_0$ is available the solutions for $p < p_0$ can be obtained very inexpensively. This is because stiffness matrices and load vectors have *hierarchic* structure [17]. Consequently the marginal cost associated with obtaining stress intensity factors for $p < p_0$ is very small. This is not the case when the h-version of the finite element method is used.

Development of theories for the prediction of failure in metallic and nonmetallic materials is a problem of very obvious practical importance. Several failure theories have been proposed, each requiring computation of some parameters of the elastic stress field (see, for example [26-31]). In linear elastic fracture mechanics the amplitude of the first symmetric term of the asymptotic expansion of the solution about the crack tip have been correlated with crack extension through laboratory experiments. It is conceivable that much like crack extension, failure initiation (e.g. the formation of cracks at weldments and reentrant corners; the onset of delamination in composite materials, etc.) can be correlated with the amplitudes of the terms of asymptotic expansions also. In fact, linear elasticity cannot be useful for predicting failure initiation events unless parameters of the elastic solution can be consistently correlated with occurrences of such events. Certain parameters can be computed only by extraction methods. Others can be computed directly from the finite element solution [32]. We have shown that accurate and inexpensive determination of the amplitudes of asymptotic expansions in the neighborhood of reentrant corners is possible.

7. ACKNOWLEDGEMENTS.

The writers wish to thank the Air Force Office of Scientific Research and the Office of Naval Research for having provided partial support for the investigation reported herein through research grants AFOSR 82-0315 and ONR-N-00014-85-K-0169, respectively. The writers also wish to thank Noetic Technologies Corporation of St. Louis, Missouri for having provided computer facilities through a collaborative research agreement with Washington University.

8. REFERENCES.

[1] Babuška, I. and Szabó, B., "On the Rates of Convergence of the Finite Element Method", Int. J. num. Meth. Engng., Vol. 18, pp. 323-341 (1982)

[2] Babuška, I., Gui, W. and Szabó, B. A., "Performance of the h, p and h-p Versions of the Finite Element Method", *Research in Structures and Dynamics*, R. J. Hayduk and A. K. Noor, editors, *NASA* Conference Publication 2335, pp. 73-93 (1984)

[3] Gui, W., "The h-p Version of the Finite Element Method for One Dimensional Problem" Doctoral Dissertation, University of Maryland, (1985)

[4] Guo, B. and Babuška, I., "The h-p Version of the Finite Element Method. Part I: Basic Approximation Results. Part II: General Results and Applications" To appear in: Comp. Mech., Springer Int.'l (1986)

[5] Szabó, B., "Estimation and Control of Error Based on P-Convergence" in: I. Babuška, J. Gago, E. R. de A. Oliveira and O. C. Zienkiewicz, editors, *Accuracy Estimates and Adaptive Refinements in Finite Element Computations*, John Wiley & Sons Ltd., pp. 61-78 (1986)

[6] Szabó, B. A., "Implementation of a Finite Element Software System with h- and p-Extension Capabilities", in: H. Kardestuncer, ed. Proc., 8th Invitational UFEM Symposium: Unification of Finite Element Software Systems, The University of Connecticut, May 1985

[7] Szabó, B. A., "Mesh Design for the p-Version of the Finite Element Method", Report WU/CCM-85/2, Center for Computational Mechanics, Washington University (1985). To appear in: *Computer Methods in Applied Mechanics and Engineering* in 1986

[8] Babuška, I. and Suri, M., "The Optimal Convergence Rate of the p-Version of the Finite Element Method", Technical note BN-1045, Laboratory for Numerical Analysis, Institute for Physical Science and Technology, University of Maryland (October, 1985)

[9] Babuška, I. and Miller, A., "The Post-Processing Approach in the Finite Element Method - Part 1: Calculation of Displacements, Stresses and Other Higher Derivatives of the Displacements", Int. J. num. Meth. Engng., Vol. 20, pp. 1085-1109 (1984a)

[10] Babuška, I. and Miller, A.,"The Post-Processing Approach in the Finite Element Method - Part 2: The Calculation of Stress Intensity Factors", Int. J. num. Meth. Engng., Vol. 20, pp. 1111-1129 (1984b)

[11] Babuška, I. and Miller, A., "The Post-Processing Approach in the Finite Element Method - Part 3: A-Posteriori Error Estimates and Adaptive Mesh Selection", Int. J. num. Meth. Engng., Vol. 20, pp. 2311-2324 (1984c)

[12] Karp, S. N. and Karal, F. C., "The Elasitic-Field Behavior in the Neighborhood of a Crack of Arbitrary Angle", Communications on Pure and Applied Mathematics, Vol. XV, pp. 413-421 (1962)

[13] Kondratev, V. A., "Boundary Problems for Elliptic Equations in Domains with Conical or Angular Points", Transactions of the Moscow Mathematical Society, Vol. 16, pp. 227-313 (1967)

[14] Melzer, H. and Rannacher, R., "Spannungskonzentrationen in Eckpunkten der Kirchhoffschen Platte", Bauingenieur, Vol. 55, pp. 181-184 (1980)

[15] Muskhelishvili, N. I., "Some Basic Problems of the Mathematical Theory of Elasticity", Published in Russian in 1933, English translation of the 3rd edition: P. Noordhoff Ltd., Groningen, Holland (1953)

[16] Williams, M. L., "Stress Singularities Resulting from Various Boundary Conditions in Angular Corners of Plates in Extension" J. Appl. Mech. ASME, pp. 526-528 (1952)

[17] Szabó, B. A., *PROBE: Theoretical Manual*, Noetic Technologies Corp., St. Louis, Missouri (1985)

[18] Izadpanah, K., "Computation of the Stress Components in the P-Version of the Finite Element Method", Doctoral Dissertation, Washington University (1984)

[19] Vasilopoulos, D., "Treatment of Geometric Singularities with the P-Version of the Finite Element Method", Doctoral Dissertation, Washington University (1984)

[20] Paris, P. C. and Sih, G. C., "Stress Analysis of Cracks", ASTM STP 381, pp. 30-81 (1970)

[21] Sha, G. T. and Yang, C-T., "Weight Function Calculations for Mixed-Mode Fracture Problems with the Virtual Crack Extension Technique", Engineering Fracture Mechanics, Vol. 21, pp. 1119-1149 (1985)

[22] Andersson, B., Private communication: Memorandum FFAP-H-736, The Aeronautical Research Institute of Sweden, March 19, 1985

[23] Rybicki, E. F. and Kanninen, M. F., "A Finite Element Calculation of Stress Intensity Factors by a Modified Crack Closure Integral" Engineering Fracture Mechanics, Vol. 9, pp. 931-938 (1977)

[24] Dempsey, J. P. and Sinclair, G. B., "On the Singular Behavior at the Vertex of a Bi-Material Wedge", Journal of Elasticity, Vol. 11, pp. 317-327 (1981)

[25] Babuška, I. and Rank, M., "An Expert System-like Feedback Approach in the h-p Version of the Finite Element Method", Technical Note, Laboratory for Numerical Analysis, Institute for Physical Science and Technology, University of Maryland (April, 1986)

[26] Whitney, J. M. and Nuismer, R. J., "Stress Fracture Criteria for Laminated Composites Containing Stress Concentrations", J. Composite Materials, Vol. 8, pp. 253-265 (1974)

[27] Nuismer, R. J. and Whitney, J. M., "Uniaxial Failure of Composite Laminates Containing Stress Concentrations", ASTM-STP 593, American Society for Testing Materials, p. 117 (1975)

[28] Potter, R. T., "On the Mechanism of Tensile Fracture in Notched Fibre Reinforced Plastics", Proc. Roy. Soc., A361 pp. 325-341 (1978)

[29] Nuismer, R. J. and J. D. Labor, "Applications of Average Stress Failure Criterion: Part I - Tension", J. Composite Materials, Vol. 12 p. 238 (1978)

[30] Nuismer, R. J., "Applications of Average Stress Failure Criterion: Part II - Compression", J. Composite Materials, Vol. 13 pp. 49-60 (1979)

[31] Mikulas, M. M., "Failure Prediction Techniques for Compression Loaded Laminates with Holes", NASA Conference Publication 2142 (1980)

[32] Szabó, B. A., "Computation of Stress Field Parameters in Areas of Steep Stress Gradients", Technical Note WU/CCM-85/1, Center For Computational Mechanics, Washington University (1985). To appear in: Communications in Applied Numerical Methods.

END

DTIC

8-86